PHYSICAL REVIEW C **82**, 061302(R) (2010)

Signatures of shape transitions in odd-A neutron-rich rubidium isotopes

R. Rodriguez-Guzman,[1] P. Sarriguren,[1] and L. M. Robledo[2]
[1]*Instituto de Estructura de la Materia, CSIC, Serrano 123, E-28006 Madrid, Spain*
[2]*Departamento de Física Teórica, Módulo 15, Universidad Autónoma de Madrid, E-28049 Madrid, Spain*
(Received 3 November 2010; published 9 December 2010)

The isotopic evolution of the ground-state nuclear shapes and the systematics of one-quasiproton configurations are studied in odd-A Rubidium isotopes. We use a self-consistent Hartree-Fock-Bogoliubov formalism based on the Gogny energy density functional with two parametrizations, D1S and D1M, and implemented with the equal-filling approximation. We find clear signatures of a sharp shape transition at $N = 60$ in both the charge radii and spin parity of the ground states, which are robust, consistent with each other, and in agreement with experiment. We point out that the combined analysis of these two observables could be used to predict unambiguously new regions where shape transitions might develop.

DOI: 10.1103/PhysRevC.82.061302 PACS number(s): 21.60.Jz, 21.10.Pc, 27.60.+j

The study of the nuclear shape evolution as the number of nucleons changes is nowadays a highly topical issue in nuclear physics from both theoretical and experimental points of view (see, for example, Refs. [1–4] and references therein). Especially interesting are those situations where the nuclear structure suffers drastic changes between neighbor nuclides. These structural variations often lead to sudden changes of particular nuclear properties that can be used as signatures of shape transitions [5,6]. This is the case of the neutron-rich isotopes with masses $A \sim 100$. Intense experimental [7–9] and theoretical [5,6,10,11] efforts are ongoing to better characterize the structural evolution of the ground and excited states in this region of the nuclear chart. In particular, we have recently studied in Refs. [5,6] the structural evolution in even and odd neutron-rich Sr, Zr, and Mo isotopes. In the present work, we concentrate on the study of neutron-rich odd-mass Rb isotopes that have received considerable attention recently [12–15] and that exemplify a general pattern where structural fluctuations lead to observable effects.

Being an odd-Z nucleus, the spin and parity of odd-A Rb isotopes are determined by the state occupied by the unpaired proton. The spectroscopic properties of the various isotopes will be determined by the one-quasiproton configurations that, in principle, are expected to be rather stable against variations in the number of even neutrons. However, as is known for neighboring nuclei, approaching $N \sim 60$ the isotopes become well deformed [1,5] and the abrupt change in deformation induces signatures in nuclear bulk properties like the two-neutron separation energies and the nuclear charge radii, as well as in spectroscopic properties. In particular, the spin and parity of the nuclear ground state might change suddenly from one isotope to another, reflecting the structural change.

We analyze in this work the bulk and spectroscopic properties of neutron-rich Rb odd isotopes within the self-consistent Hartree-Fock-Bogoliubov (HFB) approximation based on the finite range and density-dependent Gogny energy density functional (EDF) [16]. Previous studies in this region, including triaxiality [5], suggest that the γ degree of freedom would not play a significant role in these isotopes and, therefore, axial symmetry is assumed to be a self-consistent symmetry in this study.

In addition to the well known D1S parametrization [17] of the Gogny-EDF, we also consider the most recent parametrization D1M [18]. From this comparison we evaluate not only the robustness of our results, but we also explore the capability of D1M to account for the phenomenology of odd-A nuclei, which are not yet so well studied. The description of the odd-A nuclei involves additional difficulties because the blocking procedure requires the breaking of time-reversal invariance, making the calculations arduous [19,20]. In the present study we use the equal-filling approximation (EFA), a prescription widely used in mean-field calculations to preserve the advantages of time-reversal invariance. In this approximation, the odd nucleon sits half in a given orbital and half in its time-reversed partner. The microscopic justification of the EFA is based on standard ideas of quantum statistical mechanics [21]. The predictions arising from various treatments of the blocking have been studied in Ref. [22], which concluded that the EFA is sufficiently precise for most practical applications. More details of our procedure can be found in Ref. [6].

The proton and neutron single-particle energies (SPEs) are shown in Fig. 1 as a function of the axial quadrupole moment Q_{20} for the even-even ^{98}Sr ($Z = 38$, $N = 60$) isotope. Fermi levels are plotted with thick dashed (red) lines. Asymptotic (Nilsson) quantum numbers $[N, n_z, \Lambda]K^\pi$ are also shown in the proton case for the Q_{20} values where the energy minima are located (vertical arrows) in both oblate and prolate sectors. As one can see, the valence protons occupy the $N = 3$ shell and, if deformed, they start to fill the $g_{9/2}$ orbitals coming down from the $N = 4$ shell. Neutrons occupy states belonging to the $N = 4$ shell and, upon approaching $N = 60$, they start to populate the $h_{11/2}$ intruder orbitals coming down from the $N = 5$ oscillator shell at large deformations ($Q_{20} \sim 4$ to 5 b). These neutrons polarize the protons and drive them to populate the $1g_{9/2}$ shell at similar deformations. Thus, the underlying nuclear structure in this mass region is very sensitive to the occupancy of these single-particle orbitals, and the result is a rapid change in the nuclear deformation and in the spectroscopic properties as a function of both neutron and proton numbers.

In particular, Rb isotopes approaching $N = 60$ will jump abruptly from slightly deformed oblate or prolate shapes to

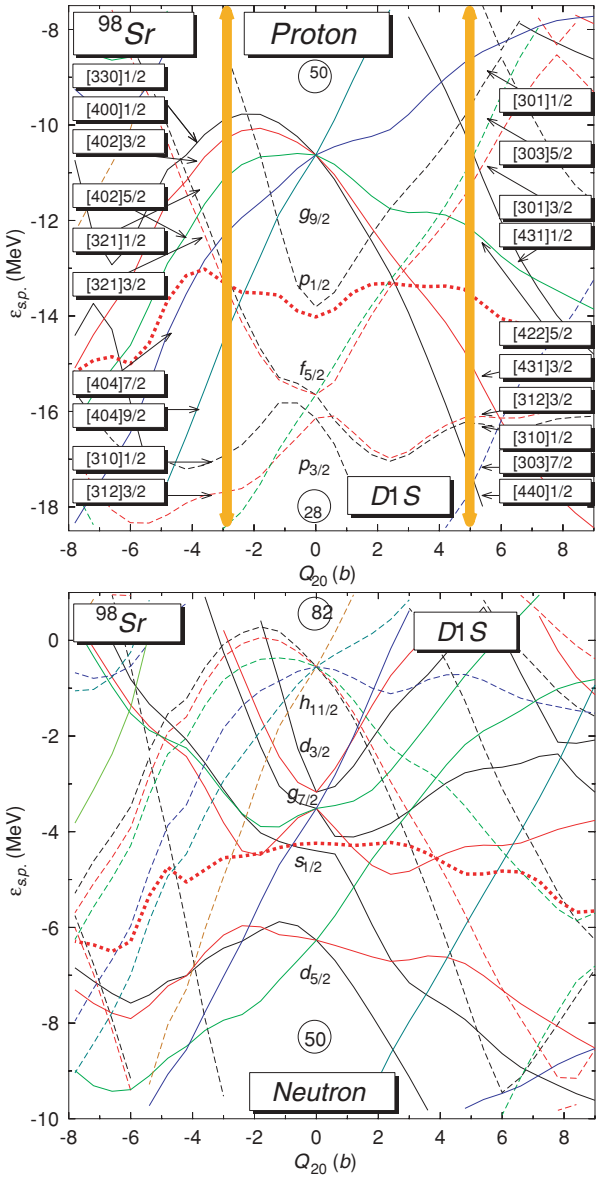

FIG. 1. (Color online) Single-particle energies for protons and neutrons in ^{98}Sr as a function of the axial quadrupole moment Q_{20}. The Fermi level is depicted as a thick dashed red line. The results have been obtained with the Gogny-D1S EDF.

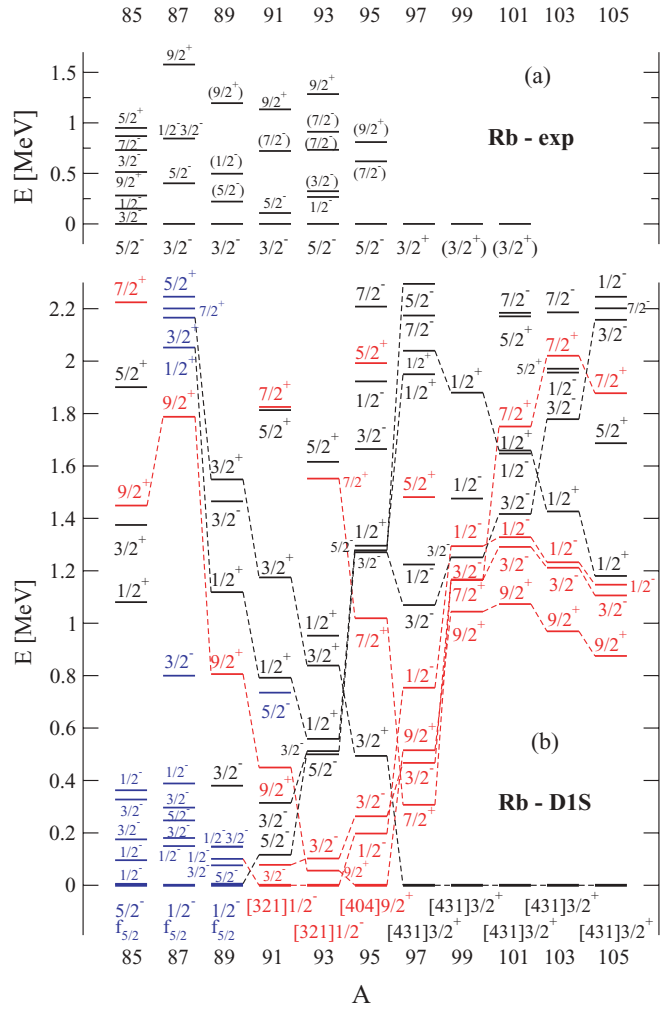

FIG. 2. (Color online) Experimental (a) excitation energies and spin-parity assignments [12–15,23] compared with Gogny-D1S HFB-EFA results (b) for one-quasiproton states in odd-A Rb isotopes. Prolate configurations are shown by black lines, oblate ones by red lines, and spherical ones by blue lines.

strongly prolate shapes. As a consequence, the unpaired proton that finally determines the spin and parity of the whole nucleus in Rb isotopes will jump from the $[303]5/2^-$ orbital at low deformation to the $[431]3/2^+$ orbital at large deformation. This is fully consistent with the Jahn-Teller picture, which states that nuclei avoid regions with high single-particle level densities around the Fermi level, thus favoring deformations where the energy gaps are higher. One sees large energy gaps at large prolate deformations for the $[431]3/2^+$ orbital. This is also consistent with the Federman-Pittel mechanism [24], which points to the $T = 0$ neutron-proton interaction as the driving force for quadrupole deformation. This force is particularly intense between spin-orbit partners (neutron $1g_{7/2}$ and proton $1g_{9/2}$ in our case), as well as between orbitals with the same radial quantum numbers and large orbital angular momenta differing by one unit $n_p = n_n$ and $\ell_p = \ell_n \pm 1$ (neutron $1h_{11/2}$ and proton $1g_{9/2}$ in our case).

In Fig. 2 we can see the experimental excitation energies and spin-parity assignments (a) in odd-A neutron-rich Rb isotopes. They are compared to the one-quasiproton states predicted by the Gogny-D1S HFB-EFA calculation (b). The excited states for a given isotope are referred to the corresponding ground state, regardless of its shape. Prolate configurations in our calculations are shown by black lines, oblate ones by red lines, and spherical ones by blue lines. The quasiparticle states are labeled by their K^π quantum numbers. The most important configurations are joined by dashed lines following the isotopic evolution. In addition, the ground states are labeled by their asymptotic quantum numbers.

Experimentally [12–15,23], one observes $J^\pi = 3/2^-$ ground states in ^{87,89,91}Rb, then $5/2^-$ states in ^{93,95}Rb, and finally $3/2^+$ states in the heavier isotopes. The $9/2^+$ states appear all the way up to ^{95}Rb as excited states. The most

striking feature observed is a jump at $N = 60$ ($A = 97$) from the $5/2^-$ to $3/2^+$ ground states.

The theoretical interpretation of these features can be understood from the analysis of our results in the lower panel (b). Rb isotopes evolve from spherical shapes in $^{85-89}$Rb around $N = 50$ with the spherical $f_{5/2}$, $p_{3/2}$, and $p_{1/2}$ shells involved to slightly deformed shapes (oblate and prolate almost degenerate) in $^{91-95}$Rb and, finally, to well-deformed prolate shapes in $^{97-105}$Rb. In the lighter isotopes the three spherical shells mentioned above are very close in energy and, thus, we can see all the split K^π levels coming from them at very close low-lying excitation energies. In the case of $^{91-95}$Rb isotopes, we obtain oblate ground states with both oblate and prolate low-lying excited states very close in energy. For instance, we see that the experimental $3/2^-$ ground states in ^{89,91}Rb appear in the calculation as excited states at less than 0.1 MeV. In the case of ^{93,95}Rb, the experimental ground states $5/2^-$ appear as prolate excited states, while the calculations produce oblate ground states. The ground states of the heavier isotopes are predicted to be $3/2^+$, in agreement with experiment. The calculations also predict excited low-lying $9/2^+$ states with an oblate nature, which are observed experimentally.

In the next figures we compare the spectroscopic properties of the Gogny D1S and D1M parametrizations. Contrary to Fig. 2, in Fig. 3 for D1S and in Fig. 4 for D1M, we have separated the prolate (a) and oblate (b) states and have plotted the most relevant hole states below zero energy and the particle states above. The absolute ground states, either oblate or prolate, are indicated with circles. Specifically, in the

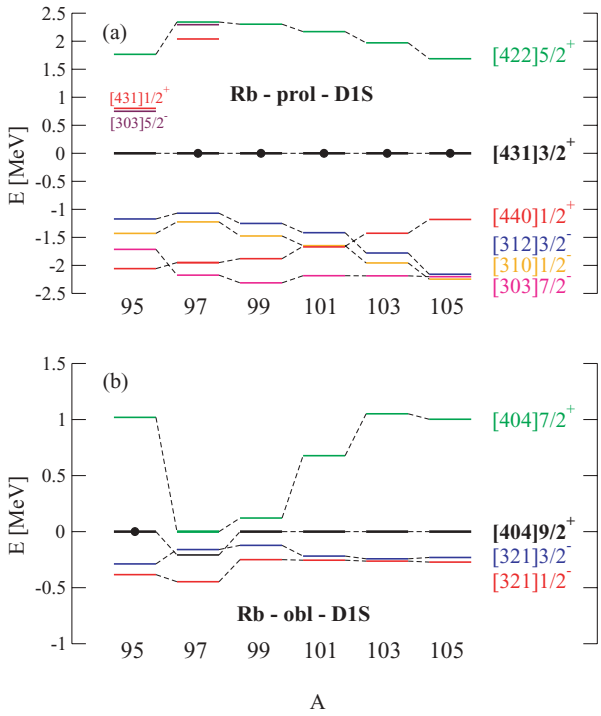

FIG. 3. (Color online) Gogny-D1S excitation energies of single-quasiproton prolate (a) and oblate (b) states in Rb isotopes. Hole states are plotted below zero energy and particle states are plotted above. The absolute ground states are indicated with circles.

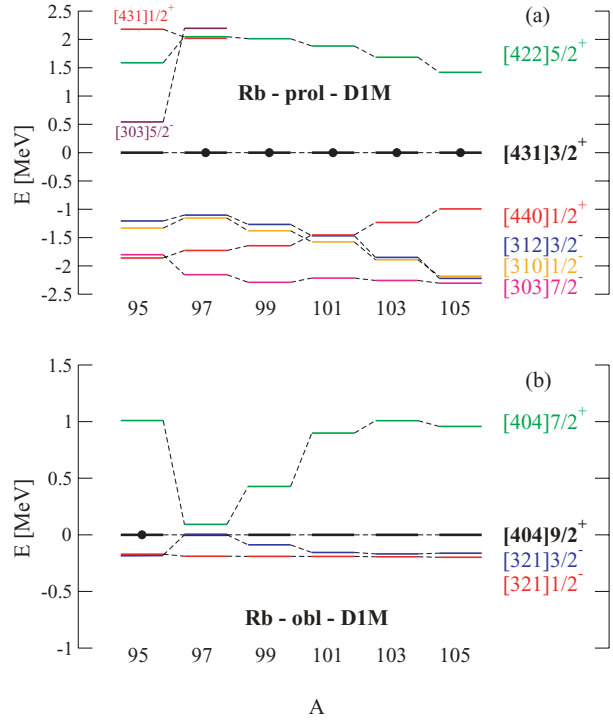

FIG. 4. (Color online) Same as in Fig. 3, but for Gogny D1M.

figures corresponding to the prolate shape, we have plotted the evolution of the $3/2^+(g_{9/2})$ states, which are ground states for $^{97-105}$Rb. In the upper region we find the $5/2^+(g_{9/2})$ state, while in the lower region we have the $1/2^+(g_{9/2})$, $3/2^-(p_{3/2})$, $1/2^-(f_{5/2})$, and $7/2^-$ states coming up from the $f_{7/2}$ shell. In the oblate case (b) we can see the $9/2^+(g_{9/2})$ state, which is the ground state in ^{95}Rb, the $7/2^+(g_{9/2})$ as a particle state, and the $1/2^-$ and $3/2^-$ from $f_{5/2}$ as hole states.

Very similar results are obtained from both parametrizations, which answer our original questions about the robustness of the calculations and the reliability of D1M. The only difference worth mentioning is that D1M produces slightly lower excited states. This feature can be understood from its larger effective mass that makes the single-particle spectrum somewhat more dense with D1M.

To further illustrate the role of deformation and spin-parity assignments in the isotopic evolution, we display in Fig. 5 the axial quadrupole deformation β of the energy minima as a function of N with both D1S and D1M parametrizations. The deformation of the ground state for each isotope is encircled. We can see that, starting at the semi-magic isotope with $N = 50$, we get two minima in the prolate and oblate sectors. These are $5/2^-$ in the prolate case and $1/2^-$ (or $9/2^+$ very close in energy) in the oblate case. The calculations with the two forces predict oblate ground states, but with prolate solutions which are very close in energy and that could perfectly well become ground states for slightly different types of calculations. Thus, in ^{89}Rb, the $1/2^-$ and $5/2^-$ states are practically degenerate (see Fig. 2). In ^{91}Rb (^{93}Rb) they are separated by less than 0.2 (0.5) MeV. The experimental information seems to favor prolate solutions since $5/2^-$ ground states are observed. The ground states of heavier isotopes

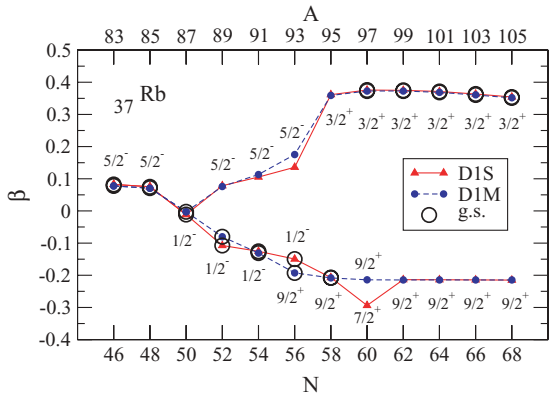

FIG. 5. (Color online) Isotopic evolution of the quadrupole deformation parameter β of the energy minima obtained from Gogny D1S and D1M calculations.

starting at ^{97}Rb are $3/2^+$, in agreement with experiment, and strongly prolate. The $9/2^+$ oblate configurations appear all the way toward heavier isotopes.

Finally, we show in Fig. 6 for D1S and in Fig. 7 for D1M, the charge radii differences (a) defined as $\delta\langle r_c^2\rangle^{50,N} = \langle r_c^2\rangle^N - \langle r_c^2\rangle^{50}$, calculated with the same corrections as in Ref. [5], and the two-neutron separation energies S_{2n} (b). We compare our results for $\delta\langle r_c^2\rangle$ with isotope shifts from laser spectroscopy experiments [27] and our results for S_{2n} with masses from Refs. [25,26]. The results for S_{2n} agree, in general, with the measurements and are very similar between D1S and D1M. A somewhat better agreement is found with D1M at the beginning of the shell ($N > 50$). In any case, it would be interesting to see whether the incipient experimental tendency to raise the S_{2n} values in the heavier isotopes—not predicted by the calculations—still persists in more exotic nuclei. In this respect, we should remark that, for the heavier Rb isotopes, the

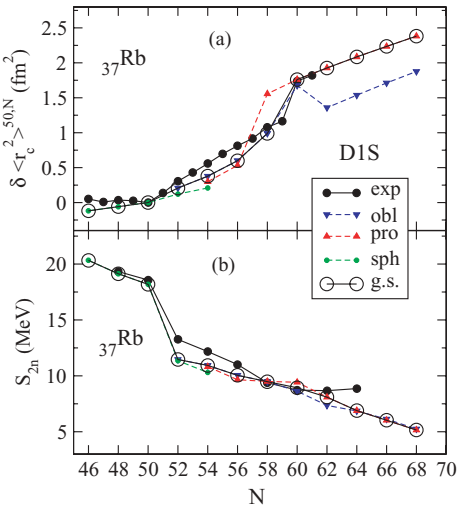

FIG. 6. (Color online) Gogny-D1S HFB results for $\delta\langle r_c^2\rangle$ (a) and S_{2n} (b) in odd-A Rb isotopes compared to experimental data from Refs. [25,26] for masses and from Ref. [27] for radii. Results for prolate, oblate, and spherical minima are displayed with different symbols (see legend). Open circles correspond to ground-state results.

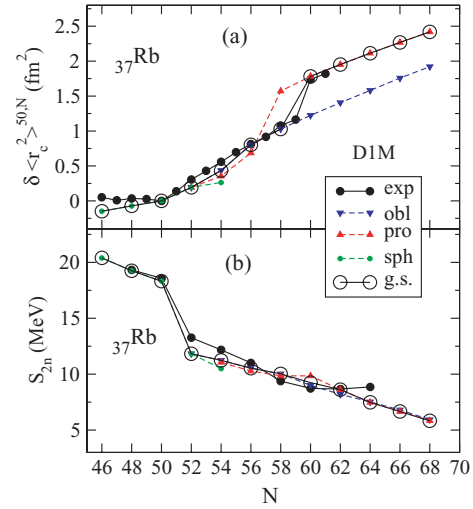

FIG. 7. (Color online) Same as in Fig. 6, but for Gogny D1M.

mass data are not completely reliable because they are based on β-endpoint measurements. It has been shown that this type of indirect measurements systematically tend to underestimate the Q values, leading to very strong binding. This problem has been discussed in Ref. [28] for neutron-rich Y and Nb isotopes. Thus, it would be very helpful to extend and improve mass measurements to reduce the still large uncertainties in neutron-rich Rb isotopes.

The nuclear charge radii plotted in the upper figures show a jump at $N = 60$, where the radius suddenly increases. This experimental observation is well reproduced in our calculations, where the encircled ground states show that the jump occurs between $N = 58$ and $N = 60$. This jump correlates well with the one observed in the spin parity of the ground states displayed in Fig. 2 from $5/2^-$ to $3/2^+$. Theoretically, the jump in $\delta\langle r_c^2\rangle$ could be understood as the result of the change from an oblate to a prolate shape. But it could also be interpreted as a jump from a slightly prolate shape to a well-deformed prolate nucleus, because the oblate and prolate shapes in the transitional nuclei $N = 54$ to 58 have very similar absolute values of deformation (see Fig. 5). This similarity gives rise to practically the same charge radii, as can be seen by comparing the prolate (upward red triangles) and oblate (downward blue triangles) radii in this region. The only difference worth mentioning between D1S and D1M is the oblate radii at $N = 60$, which corresponds to different configurations ($7/2^+$ in D1S and $9/2^+$ in D1M) and different deformations (see Fig. 5).

Then, we see that, contrary to S_{2n} which does not signal any clear signature in Rb isotopes, $\delta\langle r_c^2\rangle$ clearly indicates the existence of a shape transition, in agreement with experiment, and is well correlated to the spin-parity jump. It would also be very interesting to extend the isotope-shift measurements, which are rather old, to more exotic isotopes to also confirm the prolate stabilization.

In summary, we have studied the shape evolution in odd-A Rb isotopes from microscopic self-consistent Gogny-EDF HFB-EFA calculations. We have analyzed various sensitive nuclear observables, such as two-neutron separation energies, charge radii, and the spin parity of ground states in a

search for signatures of shape transitions. We have found that, although the masses are not very sensitive to these shape changes in Rb isotopes, the charge radii and the spin parity are. In addition, the signatures found are all consistent with each other and point unambiguously to the existence of a shape transition. The correlations between all of these signatures are useful to establish a protocol to look for shape transitions in the future in other regions of the nuclear chart and to predict and identify them. We have also analyzed the isotopic evolution of the one-quasiproton configurations and have compared the predictions of two different Gogny-EDF parametrizations, demonstrating the robustness of our calculations.

The experimental information available in neutron-rich Rb isotopes and, in general, in this mass region is still very limited. It would be highly desirable to extend the experimental programs for mass, charge radii, and spectroscopic measurements to these exotic regions at existing facilities like the tandem Penning trap mass spectrometer (ISOLTRAP) [29] at the On-Line Isotope Mass Separator (ISOLDE) facility at CERN and the Ion Guide Isotope Separator On-Line (IGISOL) facility [30] at the University of Jyväskylä, or at future ones like the precision measurements of very short-lived nuclei using an advanced trapping system for highly-charged ions (MATS) and laser spectroscopy (LaSpec) [3] at the Facility for Antiproton and Ion Research (FAIR), where we can learn much about structural evolution in nuclear systems.

The theoretical efforts should be also pushed forward by improving the formalism including triaxial degrees of freedom in those regions where this can be an issue or by dealing with the odd systems with exact blocking treatments. The quality of our mean-field description could be improved from configuration-mixing calculations in the spirit of the generator coordinate method with the quadrupole moment as the generator coordinate. Nevertheless, such an approach for odd nuclei is out of the scope of the present study. It is already known [31] that such a configuration mixing reduces the jump in S_{2n} predicted in pure mean-field approximations when crossing shell closures, improving the agreement with experiment. This could be particularly relevant for the light isotopes considered in the present study, where the spherical minima are rather shallow. For heavier isotopes, the two minima, oblate and prolate, are separated by spherical barriers of about 3 MeV and appear about 1 MeV apart. The effect here is not expected to be significant because a single shape would be enough to account for the properties studied. A simple two-state mixing model could be used to mix the intrinsic deformed configurations into the physical states [1]. Assuming that the wave functions are localized at largely different values of the deformation coordinate, one can neglect the cross terms. The final effect would be to place the value of the radius in between the oblate and prolate values according to the mixing amplitude of those intrinsic configurations in the physical wave function. The consequence would be a slightly smoother transition.

This work was supported by MICINN (Spain) under research grants FIS2008-01301, FPA2009-08958 and FIS2009-07277, as well as by Consolider-Ingenio 2010 Programs CPAN CSD2007-00042 and MULTIDARK CSD2009-00064. We thank Prof. J. Äysto and Prof. P. M. Walker for valuable suggestions and discussions.

[1] J. L. Wood *et al.*, Phys. Rep. **215**, 101 (1992).
[2] M. Bender, P.-H. Heenen, and P.-H. Reinhard, Rev. Mod. Phys. **75**, 121 (2003).
[3] D. Rodríguez *et al.*, Eur. Phys. J. Special Topics **183**, 1 (2010).
[4] R. Rodríguez-Guzmán and P. Sarriguren, Phys. Rev. C **76**, 064303 (2007); P. Sarriguren, R. Rodríguez-Guzmán, and L. M. Robledo, *ibid.* **77**, 064322 (2008); L. M. Robledo, R. R. Rodríguez-Guzmán, and P. Sarriguren, *ibid.* **78**, 034314 (2008); L. M. Robledo, R. Rodríguez-Guzmán, and P. Sarriguren, J. Phys. G: Nucl. Part. Phys. **36**, 115104 (2009); R. Rodríguez-Guzmán, P. Sarriguren, L. M. Robledo, and J. E. García-Ramos, Phys. Rev. C **81**, 024310 (2010).
[5] R. Rodríguez-Guzmán, P. Sarriguren, L. M. Robledo, and S. Perez-Martin, Phys. Lett. B **691**, 202 (2010).
[6] R. Rodríguez-Guzmán, P. Sarriguren, and L. M. Robledo, Phys. Rev. C **82**, 044318 (2010).
[7] W. Urban *et al.*, Nucl. Phys. A **689**, 605 (2001).
[8] P. Campbell *et al.*, Phys. Rev. Lett. **89**, 082501 (2002).
[9] F. C. Charlwood *et al.*, Phys. Lett. B **674**, 23 (2009).
[10] J. Skalski, S. Mizutori, and W. Nazarewicz, Nucl. Phys. A **617**, 282 (1997).
[11] F. R. Xu, P. M. Walker, and R. Wyss, Phys. Rev. C **65**, 021303 (2002).
[12] G. Lhersonneau, B. Pfeiffer, H. Gabelmann, and K.-L. Kratz, Phys. Rev. C **63**, 054302 (2001).
[13] D. Bucurescu *et al.*, Phys. Rev. C **76**, 064301 (2007).
[14] J. K. Hwang *et al.*, Phys. Rev. C **80**, 037304 (2009).
[15] G. S. Simpson *et al.*, Phys. Rev. C **82**, 024302 (2010).
[16] J. Dechargé and D. Gogny, Phys. Rev. C **21**, 1568 (1980).
[17] J. F. Berger, M. Girod, and D. Gogny, Nucl. Phys. A **428**, 23c (1984).
[18] S. Goriely, S. Hilaire, M. Girod, and S. Péru, Phys. Rev. Lett. **102**, 242501 (2009).
[19] T. Duguet, P. Bonche, P.-H. Heenen, and J. Meyer, Phys. Rev. C **65**, 014310 (2001).
[20] L. Bonneau, P. Quentin, and P. Möller, Phys. Rev. C **76**, 024320 (2007).
[21] S. Perez-Martin and L. M. Robledo, Phys. Rev. C **78**, 014304 (2008).
[22] N. Schunck *et al.*, Phys. Rev. C **81**, 024316 (2010).
[23] Evaluated Nuclear Structure Data Files (ENSDF): [www.nndc.bnl.gov/ensdf].
[24] P. Federman and S. Pittel, Phys. Lett. B **69**, 385 (1977); Phys. Rev. C **20**, 820 (1979).
[25] G. Audi, A. H. Wapstar, and C. Thibault, Nucl. Phys. A **729**, 337 (2003).
[26] S. Rahaman *et al.*, Eur. Phys. J. A **32**, 87 (2007).
[27] C. Thibault *et al.*, Phys. Rev. C **23**, 2720 (1981).
[28] U. Hager *et al.*, Nucl. Phys. A **793**, 20 (2007).
[29] M. Mukherjee *et al.*, Eur. Phys. J. **35**, 1 (2008).
[30] A. Jokinen *et al.*, Int. J. Mass Spectrom. **251**, 204 (2006).
[31] M. Bender, G. F. Bertsch, and P.-H. Heenen, Phys. Rev. C **78**, 054312 (2008).